

Silicon on sapphire mid-IR wave-front engineering by using sub-wavelength gratings

Yuewang Huang, Qiancheng Zhao, Salih K. Kalyoncu, Rasul Torun, Yumeng Lu, Ozdal Boyraz

EECS Department, University of California, Irvine, CA 92697

Author e-mail address: oboyraz@uci.edu

Abstract: We propose a methodology to manipulate reflected field for the design of wavefront engineered device in mid-IR range using sub-wavelength silicon gratings on sapphire substrate. High reflectivity mirror, blazed grating and focusing reflector are designed.

1. Introduction

Sub-wavelength high index contrast grating has been extensively investigated as a super high performance reflection surface used in quantum cascaded laser, vertical-cavity surface-emitting lasers (VCSELs), tunable VCSELs, high-Q optical resonators, low-loss hollow-core waveguides, polarization splitter [1,2]. However, the gratings in these devices were identical everywhere and only the macroscopic high reflection property of sub-wavelength grating was utilized. Recently, the grating was used to manipulate the wavefront of electromagnetic wave in sub-wavelength scale to facilitate focusing mirrors [3,4]. However, all these design are focused in visible and near-IR spectrum and no general design methodology is present. Here, we proposed a general methodology for the design of arbitrary wavefront profile. To exemplify the methodology, we demonstrate the design of conventional normal reflective mirror, blazed grating and focusing reflector at mid-IR wavelength of 4.3 μm . All the sub-wavelength gratings in this report are based on a silicon-on-sapphire platform. Silicon gratings on sapphire substrate have the advantage of both high index contrast and low loss in mid-IR[5,6].

2. Design Principles

Since the ultra-high reflectivity in high-contrast gratings are strongly related to the resonance effect in the grating grooves, the thickness of the gratings is essential to achieve high reflection efficiency in this type of sub-wavelength grating based devices. The phase delay of the reflected wave is function of the grating thickness, grating period and duty cycle as $\phi(T, p, DC)$. By properly choosing the grating thickness, one can achieve wide range of reflected phase $\phi(p, DC)$ by tuning the grating period and duty cycles while maintaining a large reflectivity. As shown in Fig. 1(a), when the silicon grating thickness is chosen to be 3.5 μm , a reflected phase variation of $>2\pi$ can be readily achieved within the region enclosed by the black solid line where the reflectivity is greater than 90%. With a manipulating range of $>2\pi$, we can theoretically design any phase profile by perturbing the geometrical parameters at different grating sites. Let's assume that the desired phase profile is an arbitrary function defined as $\phi(x) = f(x)$. Then the design procedure is to progressively and iteratively find (p_i, DC_i) pairs satisfy the phase equation in Eq. (1) subject to the restriction of high reflectivity level to maintain high power efficiency. The recursion is programmed in Matlab using the pre-computed reflectivity phase data.

$$\phi(x_i) = f\left(x_{i-1} + \frac{p_{i-1}}{2} + \frac{p_i}{2}\right) = \phi(p_i, DC_i) \quad (1)$$

We seed the recursion with a maximum reflectivity and then search for the next pair of (p_i, DC_i) closest to (p_{i-1}, DC_{i-1}) and meeting phase profile requirement. In this way, we can minimize the change between adjacent grating lines.

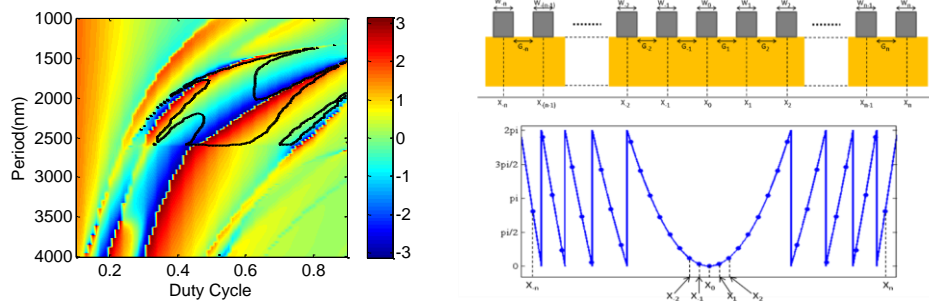


Fig. 1. (a) Phase contour for different grating periods and duty cycles for silicon-on-sapphire grating for 4.3 μm mid-IR wavelength (TM polarized, grating thickness $T=3.5\mu\text{m}$). Region enclosed by black line has a reflectivity greater than 90%. Sawtooth lines between red ($+\pi$) and blue ($-\pi$) corresponds to the phase wrapping at $\pm\pi$. Regions with red and yellow color is present twice in the black enclosure, which means $>2\pi$ phase difference can be achieved while reflectivity remains $>90\%$ (b) Schematic example showing the procedure for the design of a quadratic phase profile to deliver a focusing reflector.

3. Design Examples

First, we design a simple high efficiency reflective mirror. The phase delay function is constant across the whole region and therefore no complicated recursive is required. We just look for the maximum reflectivity for high power efficiency. Fig. 2 shows the design of a uniform grating with a period of 2.2 μm and duty cycle of 55%. Fig. 2(a) and (b) shows the magnitude and phase of the device under normal illumination from the bottom. Standing wave pattern in both the magnitude and phase show the ideal reflection mirror behavior. Due to the sub-wavelength nature of this device, only the 0-th order exists and very high efficiency is expected. The simulated reflection efficiency is nearly 100%.

Next, we show the design of a blazed grating using sub-wavelength gratings. Unlike conventional blazed gratings, the designed blazed grating is flat because all the sub-gratings in the device have the same height. The phase profile for a blazed grating has a linear phase-gradient along the X direction as expressed by Eq. 2.

$$\phi(x_i) = \phi(x_0) + \frac{2\pi}{\Lambda} x_i \quad (2)$$

Here Λ is the periodicity of the super-cell consisted of sub-gratings with different geometrical parameters. Fig. 3 shows the simulated result of a blazed grating with 6 grating sub-cells in each super-cell repeating in X direction. The periodicity is $\Lambda = 13\mu\text{m}$. Both the magnitude and phase plot shows the angled reflection. The strongest 0-th order reflection goes to an angle of 19.5° . Higher order reflections are also present.

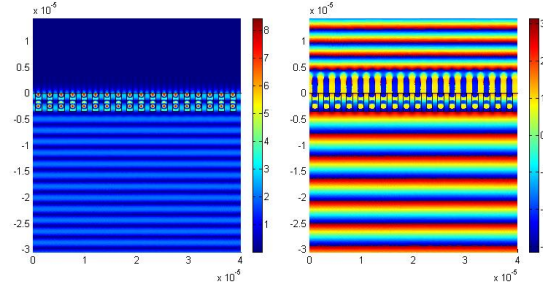


Fig. 2 Electrical field (a) magnitude and (b) phase distribution of a uniform sub-wavelength grating with a reflection efficiency of nearly 100%.

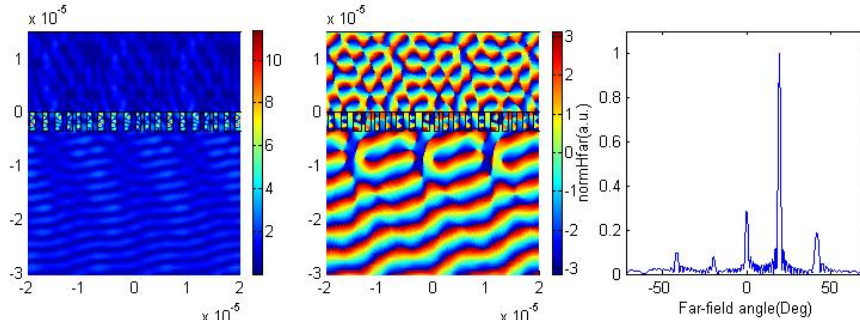


Fig. 3 (a) Magnitude and (b) phase of the blazed grating under normal TM polarized incidence from the bottom; (c) Far-field radiation of the reflected field to different angles.

The third example shows the design of a focusing reflector. The wavefront phase profile of an ideal focusing reflector is defined by Eq. 3. We use the stated design methodology to design the device. A schematic illustration of the focusing mirror is shown in Fig. 1(b).

$$\phi(x_i) = \phi(x_0) + \frac{2\pi}{\lambda} (\sqrt{F^2 + x_i^2} - F) \quad (3)$$

F is the designed focal length. Fig. 4 shows the simulation result of a design with $F = 35\mu\text{m}$. The simulated field plot clearly shows the focusing of energy to a distance of $\sim 35\mu\text{m}$. Fig. 4(b) shows that a nearly quadratic phase profile is generated and is very close to the desired phase profile. Fig. 4(c) shows the power flow on the cut-plane at the focal spot. Defraction-limited focusing is achieved and 62% of the energy is confined within the $\sim 2\mu\text{m}$ radius spot. Further optimization may still improve the power efficiency. Weak focusing can also be seen at the transmission side due to the electromagnetic duality.

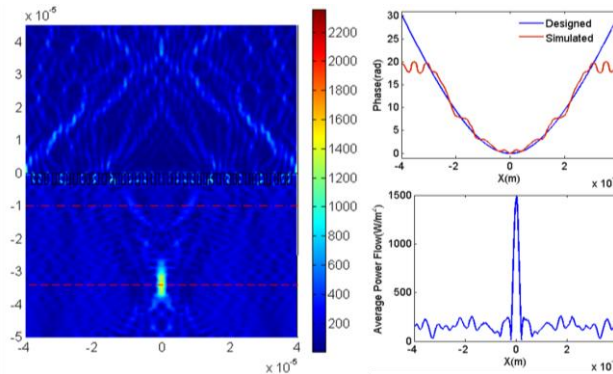


Fig. 4 (a) Full-wave power flow magnitude for the designed focusing reflector; (b) phase profile along the dash line; (c) power flow distribution along the bottom dash line through the focal point.

- [1] C.J. Chang-Hasnain and W. Yang, Adv. Opt. Photonics **4**, 379 (2012).
- [2] W. Hofmann, C. Chase, M. Muller, Y.a Rao, M.-C. Amann, & C.J. Chang-Hasnain, Photonics J. IEEE **2**, 415 (2010).
- [3] D. Fattal, J. Li, Z. Peng, M. Fiorentino, and R.G. Beausoleil, Nat. Photonics **4**, 466 (2010).
- [4] F. Lu, F.G. Sedgwick, V. Karagodsky, C. Chase, and C.J. Chang-Hasnain, Opt. Express **18**, 12606 (2010).
- [5] Y. Huang, E.K. Tien, S. Gao, S.K. Kalyoncu, Q. Song, F. Qian, & O. Boyraz, Appl. Phys. Lett. **99**, 181122 (2011).
- [6] R.A. Soref, S.J. Emelett, and W.R. Buchwald, J. Opt. Pure Appl. Opt. **8**, 840 (2006).